Bamboo wastes catalytic pyrolysis with N-doped biochar catalyst for phenols products

Wei Chen[a], Yang Fang[a], Kaixu Li[a], Zhiqun Chen[a, b], Mingwei Xia[a], Meng Gong[a], Yingquan Chen[a], Haiping Yang[a, *], Xin Tu[c] and Hanping Chen[a]

[a] State Key Laboratory of Coal Combustion, School of Power and Energy Engineering, Huazhong University of Science and Technology, Wuhan 430074, China.

[b] China-EU Institute for Clean and Renewable Energy, Huazhong University of Science and Technology, Wuhan 430074, China.

[c] Department of Electrical Engineering and Electronics, University of Liverpool, Liverpool L69 3GJ, UK.

Abstract

Biomass catalytic pyrolysis for valuable O-containing chemicals is a promising approach for better utilization of oxygen in biomass resource, where the catalyst, with the properties of green, low cost, high activity and stability, is a critical point. In this study, we proposed a novel and green method to produce phenols through biomass (bamboo wastes) catalytic pyrolysis with N-doped biochar catalyst, which was investigated in a fixed bed reactor to explore the catalytic pyrolysis mechanism of N-doped biochar catalyst. N-doped biochar catalysts, with different nitrogen content and specific surface area, were byproducts came from biomass N-enriched pyrolysis. Results showed that N-doped biochar catalyst greatly promoted the generation of phenols (reached 82%), especially valuable 4-vinyl phenol with 31% content and 6.65 wt.% yield, as well as 16% 4-ethyl phenol with 3.04 wt.% yield, based on biomass. It also promoted aromatics formation, while inhibited the generation of O-species and acetic acid with more CO_2 and H_2O release, thus greatly improved bio-oil quality. Furthermore, N-containing groups in N-doped biochar catalyst showed good stability, while O-containing groups decreased largely. N-doped biochar mainly acted as

adsorbent, catalyst, and reactant during catalytic pyrolysis, and the possible catalytic pyrolysis mechanism was proposed based on experiment results and quantum calculations. In conclusion, N-doped biochar catalyst showed excellent catalytic property for biomass catalytic pyrolysis for phenols products.

Keywords: Catalytic pyrolysis; N-doped biochar catalyst; biomass; bamboo wastes; phenols products; 4-vinyl phenol.

1. Introduction

Serious issues about energy security and environmental pollutions resulted from the excessive utilization of fossils fuels, contribute to an urgent search for renewable energy resources [1]. Biomass is regarded as one of the most potential renewable resources with huge reserve [2, 3]. Biomass pyrolysis for bio-fuel and valuable chemicals has received increasing attentions due to its low cost and environmental friendliness [4-6]. However, the heating value of typical bio-oil is only about 20 MJ/kg, which is far less than that of petroleum, due to the high content of oxygen in biomass (~50 wt.%) [7, 8]. In order to better utilization of the oxygen in biomass, lots of researchers have focused on transferring biomass into high-valued O-containing species, such as furfural, phenols, acetic acid, L-glucoseone, etc. [9, 10]. Among them, phenols are important platform compounds, which could be used for the production of phenolic resins, bisphenol A, caprolactam, as well as pharmaceutical products. However, they are mainly produced from coal or petroleum through multi-step process in industry [11, 12]. It would be greener to produce phenols from biomass.

Biomass pyrolysis could directly generate a variety of phenols, but the yield is very low [13]. Thus, to increase phenols yield, various catalysts were involved during biomass pyrolysis, mainly

including alkaline catalyst (such as KOH, K_2CO_3, NaOH, Na_2CO_3, and $Ca(OH)_2$), K_3PO_4, metal oxide (such as Fe_2O_3, Al_2O_3, ZnO, CaO, and TiO_2), and activated carbon [14, 15]. Peng et al. [16] investigated the effect of alkaline catalysts on lignin pyrolysis for phenols, and found that alkaline catalysts promoted phenols generation significantly (80% phenols in bio-oil). Lu et al. [17] pointed out that K_3PO_4 addition also enhanced the formation of phenolic enriched bio-oil. Naron et al. [15] reported that metal oxide addition was also favorable for phenols production from sugarcane lignin pyrolysis, and obtained the most significant increases of phenols with CaO and Fe_2O_3 catalysts. However, these catalysts showed alkaline corrosion or higher cost, which may be not green and cheap enough for producing phenols in large scale. In addition, Lu et al. [18] and Yang et al. [19] found that activated carbon showed good catalytic activity of biomass pyrolysis for phenols. And Zhang et al. [20], Mamaeva et al. [21], and Bu et al. [22] also reported that activated carbon significantly increased phenols content during microwave pyrolysis of biomass. However, the catalytic effect of activated carbon mainly depends on the developed pores structure, while the active sites still need to be improved to achieve better catalytic activity.

Our previous studies found that biomass pyrolysis under NH_3 atmosphere could promote the formation of phenols products, especially phenols without methoxyl [23, 24]. N-doped biochar, the byproduct of biomass pyrolysis under NH_3 atmosphere, compared with activated carbon, not only had developed porous structure, but also contained abundant active N- and O-containing groups [25, 26]. Moreover, these N-containing groups (including pyridinic-N, pyrrolic-N, quaternary-N, and pyridone-N-oxide) in N-doped biochar showed alkaline and could effectively adsorb acid gas or volatiles [27, 28]. Biomass pyrolysis generated large amounts of acid intermediates and carbonyl species, which were easy to combine with N-containing groups, thereby promoted the catalytic reactions [29]. Besides, our previous study found that active O-

containing groups in biochar could also promote the generation of non-methoxyl phenols [30]. Thus, if N-doped biochar is used as catalyst during biomass catalytic pyrolysis, it may show synergetic effect for the formation of phenols by combining the advantages of activated carbon, active functional groups, and NH_3. However, the catalytic pyrolysis of biomass with N-doped biochar catalyst for producing phenols is not reported right now.

Hence, a novel method to produce phenols through biomass catalytic pyrolysis with N-doped biochar catalyst was proposed. Besides, bamboo wastes catalytic pyrolysis with N-doped biochar catalyst was investigated, and the formation mechanism of phenols products was explored, as well as the evolution behavior of N-doped biochar catalyst during catalytic pyrolysis, to better understand the catalytic pyrolysis mechanism of N-doped biochar catalyst for producing phenols. It is important for the green and valuable utilization of biomass resource.

2. Materials and methods

2.1. Materials

Bamboo wastes were involved as biomass sample, which were collected locally. The feedstock was dried at 105°C for 24 h, then crushed and sieved to obtain a particle less than 120 μm before use. Proximate analysis of bamboo was conducted using a TGA-2000 analyzer (las Navas, Spain) according to National Standard in China GBT 28731-2012. Ultimate analysis of sample was performed in a CHNS/O elementary analyzer (Vario Micro Cube, Germany). The lower heating value (LHV) of bamboo was measured using a bomb calorimetry (Parr 6300, USA). The content of hemicellulose, cellulose and lignin in bamboo was determined by Van Soest [31, 32]. Bamboo showed high volatile content (80.57 wt.%) with only 2.32 wt.% ash (Table S1). Carbon and oxygen content reached 41.97 wt.% and 43.18 wt.%, respectively, with only 0.27 wt.%

nitrogen [24]. Besides, cellulose was the main biochemical composition (46.5 wt.%) with 18.8 wt.% hemicellulose and 25.7 wt.% lignin.

2.2. N-doped biochar catalyst preparation

N-doped biochar catalysts were derived from bamboo fast pyrolysis at 600°C for 30 min with variant NH_3 concentrations (10 vol.%, 30 vol.%, and 50 vol.%, respectively. The total flow of mixture atmosphere of Ar (99.999%) and NH_3 (99.999%) was kept at 200 mL/min). The detail preparation method used here could be found in our previous study [23]. The three N-doped biochar catalysts, with different nitrogen content and porous properties, were named as biochar-N10, biochar-N30, and biochar-N50, respectively.

2.3. Catalytic pyrolysis experiment

Catalytic pyrolysis of bamboo wastes was performed in a fixed bed system, shown as Figure 1. The system consisted of a feeding unit, a fixed bed pyrolysis reactor (600 mm height, 45 mm inner diameter), a condensing unit, and a gas cleaning and drying unit, with temperature and gas flow rate controllers.

Prior to each trial, the pyrolysis reactor was heated up to 600°C with high purity Ar purging (200 mL/min) previously (which could obtain higher yield and quality of bio-oil) [24, 30]. When the system was stable, the sample holder with biomass and N-doped biochar mixture (3 g, mass ratio of bamboo and N-doped biochar catalyst is 2:1 with same mixing method and mixing time to maintain the consistency of each experiment) was promptly placed to the centre of the reactor and kept for 30 mins [19, 30]. Biomass sample was heated up and the volatiles evolved out rapidly. The condensable volatiles were trapped in the ice-water mixture condensing unit. The non-condensing gas was dried, cleaned, and collected with gas bag for further analysis. Furthermore,

to precisely quantify the bio-oil yield and completely collect the bio-oil, each trial was replicated with liquid nitrogen condensing instead of ice-water mixture.

After each experiment, the reactor was cooled to ambient temperature with Ar purging. Biochar and bio-oil yields were determined with the weight differences of the quartz basket, liquid nitrogen condensing unit, respectively. The gas yield (wt.%) was calculated with combining the total gas volume and the gas density [30]. For comparison, biochar catalyst without doping nitrogen (named as biochar) was also prepared through bamboo pyrolysis at 600°C for 30 min with Ar atmosphere (200 mL/min) [30], to illustrate the effect of N-doped biochar catalyst. And bamboo pyrolysis without catalyst (named as without biochar) was performed at 600°C for 30 min with Ar (200 mL/min) to better illustrate the effect of catalytic pyrolysis. Besides, all experiments were run in triplicate at least with good mass balance (97.59-104.09 wt.%), and all data took the average.
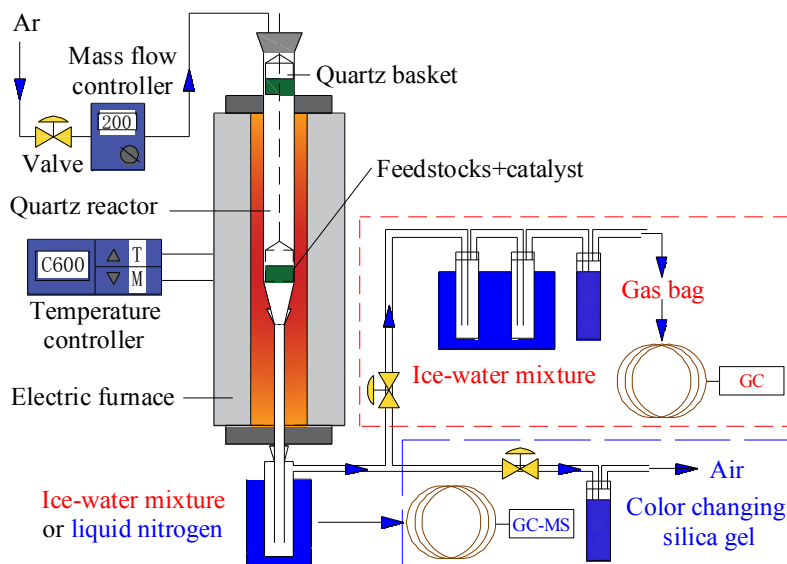

Figure 1. Schematic diagram of catalytic pyrolysis system.

2.4. Characterization

The gas products were analyzed using a dual-channel micro-gas chromatography system (Micro-GC 3000A, Agilent Technologies, USA), with thermal conductivity detectors. Two

columns were used: Column A (molecular sieve 5A, Ar carrier gas) for analyzing H_2, CO and CH_4 at 95 °C; Column B (ProapakQ-PPQ, He carrier gas) for analyzing CO_2, C_2H_6, C_2H_4, C_2H_2 at 60°C. Each sample was tested at least three times to take the average. The LHV of the gas products was determined using following equation [23]:

$$LHV(MJ/Nm^3) = 0.126 \times CO + 0.108 \times H_2 + 0.358 \times CH_4 + 0.665 \times C_nH_m \quad (1)$$

where CO, H_2, CH_4 and C_nH_m ($C_nH_m = C_2H_2 + C_2H_4 + C_2H_6$) are the volume fractions of those species.

The main compositions of bio-oil were identified using a gas chromatography-mass spectroscopy (GC-MS, HP7890 series GC with an HP5975 MS detector) with a capillary column (Agilent: HP-5MD, 19091s-433; 30 m × 0.25 mm i.d. × 0.25 μm d.f.). The injector temperature was 300°C; the carrier gas (He) flow rate for the column was 1 mL/min, and the split ratio was 20:1. In each case, a sample injection volume of 1 μL was employed. The GC oven was initially heated at 40°C for 3 min, after which time it was heated to 150°C at a rate of 5°C/min, followed by heating to 300°C at a rate of 10°C/min, and finally the oven temperature was maintained at 300°C for 10 min. The mass spectrometer was operated in a mass/charge ratio (m/z) of 30-500. Quantification of phenols product was performed with 4-vinyl phenol, 4-ethyl phenol, p-cresol, phenol by external standards through five-point method. The compounds were identified using a National Institute of Standards and Technology library (NIST2011). The water content of the bio-oil was measured by a Karl-Fischer titration (TitroLine KF-10, Schott, Germany). The pH value of the bio-oil was determined using a Starter 2100/3c Pro pH meter (Ohaus, USA).

Ultimate analysis of N-doped biochar catalyst was conducted using a CHNS/O elementary analyzer (Vario Micro Cube, Germany). Proximate analysis was carried out in a TGA-2000 analyzer (Las Navas, Spain). The surficial N- and O-containing functional groups of N-doped

biochar catalyst were analysed with X-ray photoelectron spectroscopy (XPS, Axis Ultra DLD, Kratos, UK) using Al Kα line (15 kV, 10 mA, 150 W) as a radiation source. C1*s* peak position, set at 285 eV, was used as an internal standard. The curves on C1*s* peaks were fitted by XPS peak4.1 software. The content of each element was determined by the corresponding peak area and calibrated by the atomic sensitivity factor with C as a reference.

The porous characteristics of N-doped biochar catalyst were measured using nitrogen isothermal adsorption at 77 K with an accelerated surface area and porosity system (ASAP 2020, Micromeritics, USA). Prior to the adsorption, the samples were degassed at 150 °C for 10 h. BET specific surface area (S_{BET}) was determined by the Brunauer-Emmett-Teller (BET) equation. The total pore volume (V_{total}) was determined by single point adsorption total pore volume analysis. Average pore diameter (D) was determined by $4V/S_{BET}$ based on BET method. Field emission scanning electron microscopy (FESEM, Sirion 200, FEI, Holland) was used to understand the morphology of N-doped biochar.

It should be pointed out that biomass and N-doped biochar were mixed together, and the solid char from biomass pyrolysis was mixed with N-doped biochar catalyst, and they cannot be separated. Thus N-doped biochar catalyst was considered as no mass change when biochar yield was calculated. So the yield of biochar, bio-oil and gas was determined as follows (Equations (2) to (5)):

$$\text{Biochar yield (wt. \%)} = \frac{\text{mass of soild product} - \text{mass of catalyst}}{\text{mass of feedstock}} \quad (2)$$

$$\text{Bio} - \text{oil yield (wt. \%)} = \frac{\text{mass of bio} - \text{oil}}{\text{mass of feedstock}} \quad (3)$$

$$\text{Gas yield (wt. \%)} = \frac{\text{mass of gas product}}{\text{mass of feedstock}} \quad (4)$$

$$\text{Mass balance (wt. \%)} = \text{biochar yield} + \text{bio} - \text{oil yield} + \text{gas yield} \quad (5)$$

Besides, considering possible nitrogen emission during bamboo catalytic pyrolysis with N-doped biochar catalyst, the nitrogen recovery in N-doped biochar catalyst and biochar product was also calculated. The calculating method of nitrogen recovery was that nitrogen content in N-doped biochar catalyst and biochar product after catalytic pyrolysis divided nitrogen content in N-doped biochar catalyst and bamboo feedstock before catalytic pyrolysis, shown as follows:

$$\text{Nitrogen recovery (wt. \%)} = \frac{\text{mass of nitrogen in catalyst and biochar}}{\text{mass of nitrogen catalyst and feedstock}} \quad (6)$$

In addition, to reveal the catalytic pyrolysis mechanism of bamboo with N-doped biochar catalyst, the Gaussian 09 suite of programs [33] and density functional theory (DFT) method were used here. The geometries of reactants, intermediates, transition states and products were optimized under M062X/6-311+G(d,p) level of theory. To obtain the thermodynamic parameters and assure the transition states have sole imaginary frequency while others have no imaginary frequency, frequency analysis was also conducted with the same method. Intrinsic reaction coordinate (IRC) analysis was performed to verify the transition states correlating to the correct reactants and products. Activation energies of the reactions were estimated as the free energies differences between the transition states and the reactants, including zero-point energy correction (ZPE). Free Energies were used for discussions on energetics, under the 773K and 1 atm. The reaction rate constants for rate determining steps were computed at 773K using TST with Wigner tunneling correction, as implemented in the KiSThelP program [34]. The zero-point vibrational energy was scaled with factor of 0.967 for the M062X/6-31+G(d,p) level of theory [35], which was most similar to the level of theory employed here.

3. Results and discussion

3.1. Properties of N-doped biochar catalyst

Detail information about the N-doped biochar catalyst is listed in Table 1. Biochar catalyst contained higher carbon content (84.7 wt.%) with 6.72 wt.% oxygen content. Being different with biochar, the nitrogen content of N-doped biochar catalyst increased significantly with NH_3 concentration increase, which was in the range of 1.55-3.42 wt.% [23]. And the oxygen content showed the similar tendency, which was in the range of 5.12-7.13 wt.%. Besides, the S_{BET} of biochar was only 19.16 m^2/g, while the S_{BET} of N-doped biochar also increased greatly with NH_3 concentration increase, which was in the range of 29.69-254.54 m^2/g. Moreover, they showed developed mesoporous structure with the average pore diameter of 4.26-4.79 nm. From SEM micrographs (Figure S1), it could be observed that biochar showed smooth surface without obvious porous structure. While the surface of N-doped biochar presented large amounts of pores, which could promote the pyrolytic intermediates to access the active functional groups inside the N-doped biochar [36]. With NH_3 concentration increasing, the amounts of pores increased significantly, indicating the developed porous structure. It is also consistent with the results of Table 1.

Table 1. Physicochemical properties of N-doped biochar catalyst.

Catalyst	Elemental composition, wt.%, d				Porous characteristics, d		
	N	C	H	O*	S_{BET} (m^2/g)	V_{total} (cm^3/g)	D (nm)
Biochar	-	84.70±0.03	2.48±0.02	6.72	19.16±0.23	0.075±0.005	15.58±0.26
Biochar-N10	1.55±0.01	85.02±0.01	2.49±0.03	5.12	29.69±1.12	0.036 ±0.004	4.79±0.11
Biochar-N30	1.86±0.01	83.45±0.01	2.61±0.02	6.46	83.13±3.65	0.094 ±0.008	4.51±0.12
Biochar-N50	3.42±0.01	81.29±0.02	2.43±0.01	7.13	254.54±7.48	0.271 ±0.014	4.26±0.09

d represented dry basis; O* was calculated by difference; S_{BET} represented BET specific surface area; V_{total} represented the total pore volume; D represented average pore diameter.

In addition, the O- and N-containing groups on the surface of N-doped biochar catalyst are shown in Figure 2. The O 1s spectra of catalyst was deconvoluted into four peaks (Figure 2a and 2b): carbonyl oxygen of quinines (C=O, 531.0-531.9 eV); carbonyl oxygen atoms in esters and anhydrides, and oxygen atoms in hydroxyl groups (O-C=$\underline{O}$/-OH, 532.3-532.8 eV); non-carbonyl (ether-type) oxygen atoms in esters and anhydrides ($\underline{O}$-C=O/C-O, 533.1-533.8 eV); oxygen atoms in carboxyl groups (-COOH, 534.3-535.4 eV) [30, 37, 38]. The N1s spectra of N-doped biochar was deconvoluted into four peaks (Figure 2c): pyridinic-N (398.5±0.3 eV), pyrrolic-N (399.8±0.3 eV), quaternary-N (401.2±0.3 eV) and pyridone-N-oxide (403.2±0.3 eV) [23-25].

It could be found that the main existing forms of oxygen in biochar were C=O groups with some O-C=$\underline{O}$/-OH, $\underline{O}$-C=O/-OH and -COOH groups (Figure 2a), while C=O and O-C=$\underline{O}$/-OH groups were the main O-containing groups in N-doped biochar catalyst (Figure 2b). The main existing forms of nitrogen in N-doped biochar catalyst were pyridinic-N, pyrrolic-N and quaternary-N with little pyridone-N-oxide (Figure 2c). These higher active O- and N-containing groups in N-doped biochar catalyst, with developed mesoporous structure, would have an important role in catalytic pyrolysis of biomass [39, 40]. Furthermore, different N-doped biochar catalyst showed similar distribution of O- and N-containing groups on the surface of catalyst, thus only biochar-N30 catalyst is shown here, and others are shown in Figure S2.
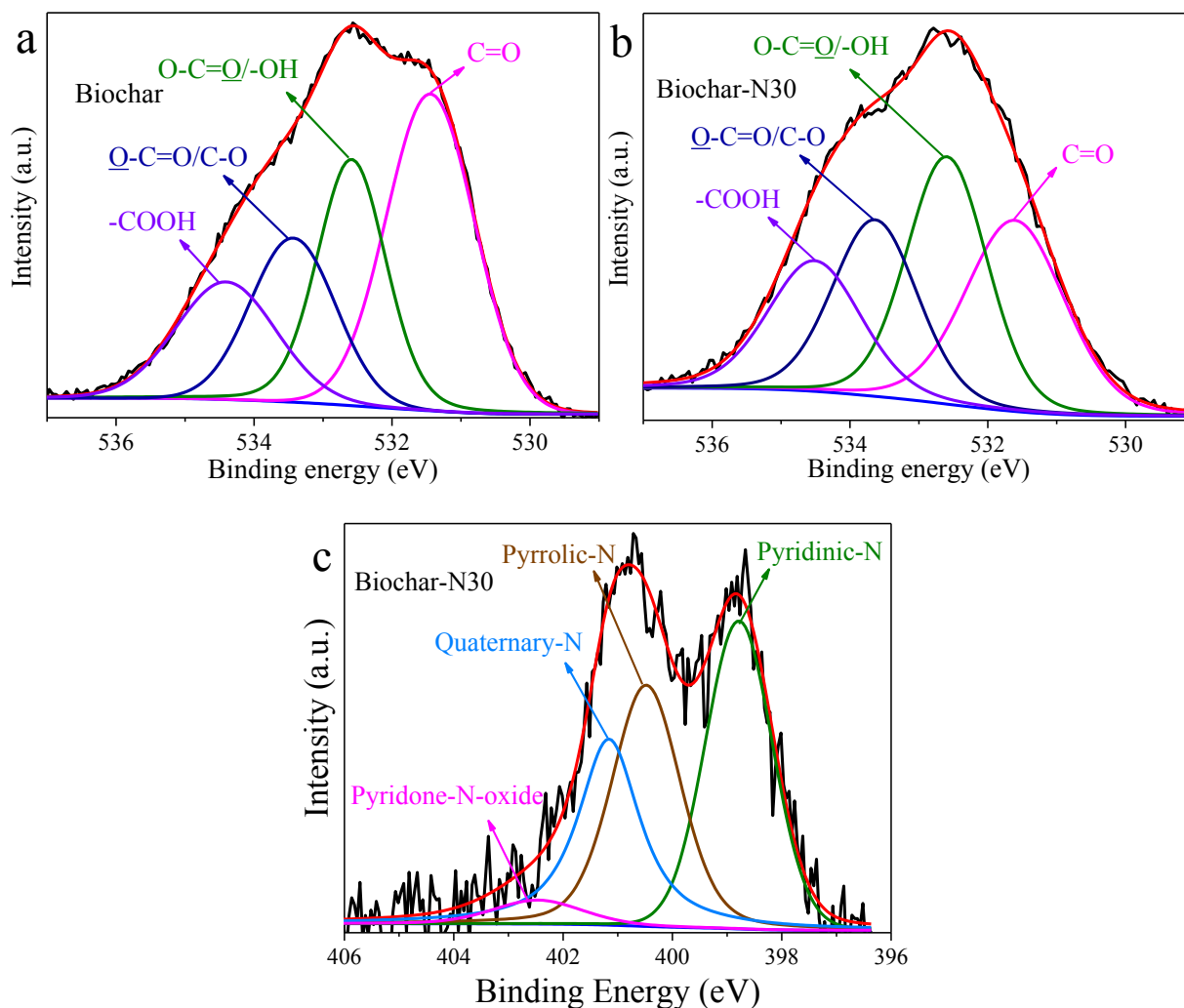
Figure 2. O- and N-containing groups in biochar (a) and N-doped biochar catalyst (b and c).

3.2. Catalytic pyrolysis properties

The products distribution from catalytic pyrolysis of bamboo is shown in Figure 3a. Bamboo pyrolysis showed higher bio-oil yield (60 wt.%), while obtained less biochar (19 wt.%) and gas product (18 wt.%). With biochar addition, bio-oil yield still maintained at 60 wt.%, while gas product yield increased significantly to 21 wt.%, as biochar addition might promote the secondary cracking of volatiles from bamboo pyrolysis and lead to more light gas formation [30]. After introducing N-doped biochar, the yield of bio-oil and gas product increased slightly further, due to the stronger catalytic reactivity of N-doped biochar [41].
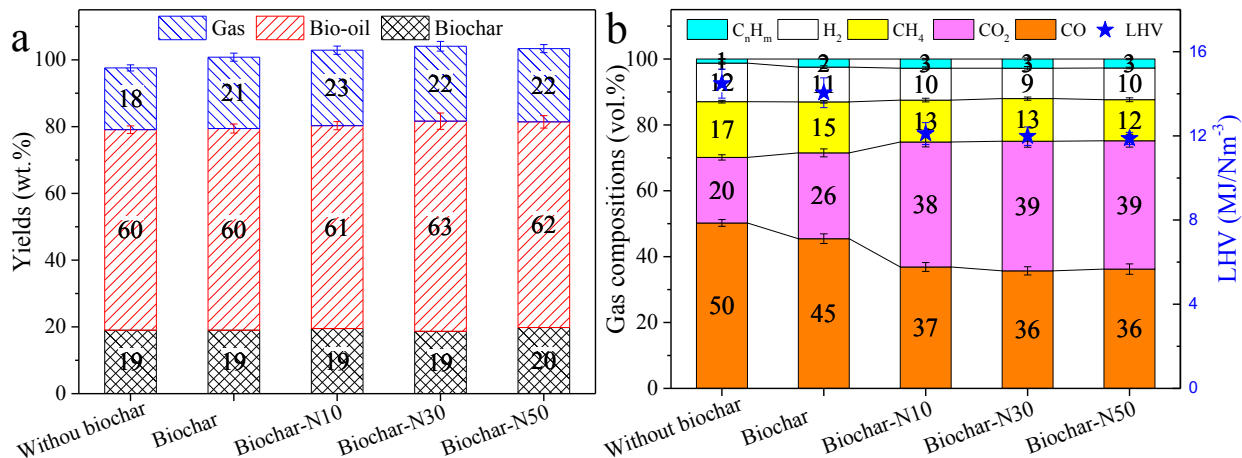
Figure 3. Production distribution (a) and gas releasing properties (b) of catalytic pyrolysis.

The releasing properties of main gaseous products (CO, CO_2, CH_4, H_2 and C_nH_m) are shown in Figure 3b. For bamboo pyrolysis, CO was the main gaseous component (50 vol.%) from the cracking of C-O-C and –C=O groups (bamboo contained large amounts of these groups) [42], with some CO_2, CH_4 and H_2. After biochar addition, CO decreased largely to 45 vol.%, while CO_2 content increased significantly to 26 vol.%, and CH_4 and H_2 decreased a little accordingly, due to the decarboxylation effect of biochar [30]. With N-doped biochar addition, CO decreased further to only 37 vol.%, while CO_2 content increased further to 38 vol.%, it might be attributed to the stronger decarboxylation reactions between O-containing pyrolytic intermediates and N-doped biochar [30]. Furthermore, the content of CH_4 and H_2 decreased largely to only 13 vol.% and 10 vol.%, respectively, which also led to the LHV of gas product decreasing from 15 to 12 MJ/Nm^3. And the NH_3 concentration during N-doped biochar preparation showed no obvious effect on gaseous components.

3.3. Properties of liquid bio-oil

The water content and pH value of bio-oil are shown in Table S2. The water content of bio-oil from bamboo pyrolysis was quite high, about 31 wt.%, which might be due to the higher oxygen content and dehydration of bamboo sample. The pH value was about 2.5, which indicated that bio-

oil showed higher acidity, and it might be corrosive during the storage and utilization process [30]. With biochar introduction, the water content (38 wt.%) and pH value (3.5) increased significantly, as biochar promoted the dehydration reactions and inhibited the formation of acid products [30]. Besides, after N-doped biochar addition, the water content increased obviously further (40 wt.%), and the pH value also increased greatly to about 4.5. It might be ascribed to that N-doped biochar addition further enhanced the dehydration reactions, and decreased the formation of acids [43]. It would significantly increase the stability of bio-oil and avoid the problem of acid corrosion during the follow-up use [44, 45].

The main organic components of bio-oil are phenols, aromatics, O-species (including furans, aldehyde, ketone, alcohol and ester), and acetic acid. The content of the main components is shown in Figure 4a. For bamboo pyrolysis, the phenol content was about 47%, with some acetic acid, furans and limited aromatics. The acetic acid content was quite high (>20%), which might explain the lower pH value of bio oil. Higher phenols from bamboo pyrolysis mainly resulted from lignin (25.7 wt.%) decomposition, while O-species and acetic acid mainly came from the cracking of cellulose and hemicellulose [46]. With biochar addition, phenols content increased significantly to 59%, while that of O-species and acetic acid decreased accordingly to 19% and 14%, respectively. It might be due to that biochar promoted the decarboxylation, dehydration, and removing alkyl branch chain of pyrolytic intermediates, leading to more phenols and less O-species and acetic acid (releasing out as CO_2) [16, 30]. It was consistent with the increase of water and pH value of bio-oil, and CO_2 content of gas product.
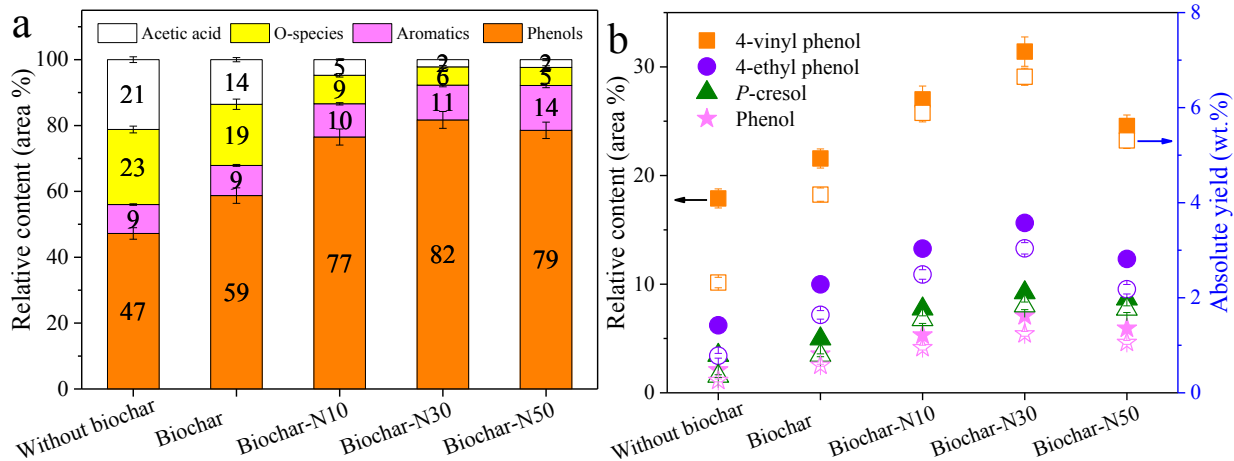
Figure 4. Bio-oil compositions of catalytic pyrolysis (a) and major phenols distribution (b). Solid represented relative content; open represented absolute yield.

With N-doped biochar introduction, phenols content increased further to 77%, while that of O-species and acetic acid decreased largely to only 9% and 5%, respectively, and aromatics content also increased gradually, indicating the stronger catalytic activity of N-doped biochar catalyst. With the increase of NH_3 concentration during N-doped biochar preparation, phenols content increased to the maximum value of 82% for biochar-N30, then it decreased gradually with NH_3 concentration increasing further. While aromatics content increased significantly and reached 14%, and the content of O-species and acetic acid decreased largely to only 5% and 2% for biochar-N50, respectively.

In particular, it could be found that the content of phenols was different with variant N-doped biochar catalysts. Phenols content increased firstly with the increase of nitrogen content (<1.86 wt.%) in N-doped biochar due to the increase of active species of catalyst. However, phenols content decreased gradually when nitrogen content of N-doped biochar increased further. It may indicate that the catalytic effect of N-doped biochar not only depended on active N-containing groups and S_{BET}, but also relied on the distribution of active species on the surface of porous structure [47]. This still needs to be investigated in depth in future work.

N-doped biochar catalyst promoted the generation of phenols (mainly simple phenols, including 4-vinyl phenol, 4-ethyl phenol, p-cresol, phenol), which may be ascribed to that: 1) Active O- and N-containing groups in N-doped biochar catalyst promoted the breaking of β-O-4 linkage to form more phenols intermediates; 2) N-doped biochar catalyst also promoted the H-donors (such as water, aldehyde, alcohol) from the decomposition of hemicellulose and cellulose reacting with phenols intermediates (H-acceptors) to form more phenols [18, 48]; 3) N-doped biochar catalyst promoted the cracking of –O-CH$_3$ in phenols intermediates to generate more simples phenols [30]; 4) N-doped biochar catalyst also promoted the decomposition of lignin, and inhibited the cracking of hemicellulose and cellulose, thus increased the content of phenols in bio-oil [49]. Besides, the decrease of O-species was mainly due to the deoxygenation effect of N-doped biochar catalyst [17]. For example, O-species intermediates provide hydrogen for the generation of phenols, which may undergo deoxygenation reactions during these process [48].

Moreover, N-doped biochar catalyst may convert ketones into aromatics through condensation and dehydration reactions, which may also transform furfurals into aromatics through multi-step reactions [50, 51]. It may be also the reason of the increase of aromatics in bio-oil. The decrease of acetic acid may be attributed to the neutralization or decarboxylation reactions of N-doped biochar catalyst [24], as the alkaline N-containing groups in N-doped biochar catalyst would easily adsorb acetic acid intermediates and react with them.

In addition, it should be pointed out that the main compounds of phenols in bio-oil were 4-vinyl phenol (a high-valued platform compound, 2500 yuan/kg), 4-ethyl phenol, p-cresol, and phenol, and the content of them is shown as Figure 4b. For bamboo pyrolysis, the yield of 4-vinyl phenol was about 18%, due to the higher lignin content of bamboo sample. With biochar introduction, it increased obviously to 22%. While with N-doped biochar addition, 4-vinyl phenol

content increased linearly, the highest content of which reached 31% (based on organic components of bio-oil) as NH_3 concentration of 30 vol.% during N-doped biochar preparation, after that it decreased obviously with NH_3 concentration increasing (50 vol.%). The content of 4-ethyl phenol, p-cresol and phenol also showed the similar tendency with that of 4-vinyl phenol. Bamboo pyrolysis only generated little of them, while their content could reach 16%, 9%, and 7% for biochar-N30, respectively. Regard to the yield of phenols, the quantification of 4-vinyl phenol, 4-ethyl phenol, p-cresol, phenol was performed, and the yield of them is shown in Figure 4b. It can be found that the yield of 4-vinyl phenol from bamboo pyrolysis was very low, only 2.32 wt.%. While with biochar addition, it was doubled to 4.17 wt.%. Furthermore, with N-doped biochar introduction, the yield of 4-VP increased linearly and reached the maximum value (6.65 wt.%, based on bamboo feedstock) with biochar-N30. After that, it decreased slightly. The yield of 4-ethyl phenol, p-cresol and phenol also presented similar tendency, which was lower than 1 wt.% from bamboo pyrolysis, while they reached 3.04 wt.%, 1.83 wt.%, and 1.24 wt.% for biochar-N30, respectively.

It should be noted that the maximum yield of valuable 4-vinyl phenol being achieved here was much higher than that of previous studies [52, 53]. It might be attributed to that 4-vinyl phenol mainly came from the cracking of p-hydroxyphenyl and methoxyl phenylpropanoid (guaiacyl and syringyl) subunits in lignin [54-56]. N-doped biochar promoted the cracking of β-O-4 in lignin, then led to the generation of more p-coumaryl, coniferyl and sinapyl alcohol subunits intermediates, thus formed more 4-vinyl phenol. Besides, N-doped biochar catalyst had the advantage of green, low cost, high activity and stability, which had the potential for large scale preparation and application for producing valuable 4-vinyl phenol product [36].

3.4. Physicochemical properties of biochar product and N-doped biochar catalyst

The physicochemical properties of N-doped biochar catalyst after catalytic pyrolysis are shown in Table 2. It should be noted that biochar or N-doped biochar catalyst was mixed together with biochar product from bamboo catalytic pyrolysis, which was difficult to be separated. However, catalyst was the main part in solid biochar, which accounted for over 70% (As biochar product yield of bamboo wastes pyrolysis without biochar was 19 wt.% (Figure 3)). Thus, to a certain extent, some properties of solid products could represent for the properties of catalyst, especially the property related to nitrogen, as almost no nitrogen in bamboo sample.

Table 2. Physicochemical properties of N-doped biochar catalyst after catalytic pyrolysis.

Catalyst	Elemental composition, wt.%, d				Porous characteristics, d		
	N	C	H	O*	S_{BET} (m^2/g)	V_{total} (cm^3/g)	D (nm)
Biochar	-	83.31±0.02	2.10±0.01	8.64	6.27±0.21	0.039±0.002	25.18±0.37
Biochar-N10	1.42±0.01	87.39±0.02	2.30±0.01	2.71	21.37±0.45	0.027±0.001	5.07±0.10
Biochar-N30	1.69±0.02	86.96±0.03	2.28±0.02	2.69	52.35±1.29	0.065±0.004	4.94±0.08
Biochar-N50	2.65±0.01	86.43±0.01	2.29±0.01	2.61	168.34±6.55	0.194±0.008	4.62±0.07

d represented dry basis; O* was calculated by difference; S_{BET} represented BET specific surface area; V_{total} represented the total pore volume; D represented average pore diameter.

Comparing the composition of biochar pre and after use, it could be found that, carbon content in biochar catalyst decreased slightly to 83 wt.% after catalytic pyrolysis, while oxygen content increased accordingly to 8.64 wt.%. It may be due to that some O-species from bamboo pyrolysis condensed on biochar catalyst surface. While for N-doped biochar, different trend displayed and carbon content increased significantly to ~87 wt.%, perhaps due to the carbon deposition during catalytic pyrolysis process [30, 57]. Accordingly, oxygen content in N-doped biochar decreased largely to only 2.7 wt.%. It may be ascribed to that active O-containing groups in catalyst reacted with pyrolytic intermediates through deoxygenation reactions, leading to the decrease of oxygen

content in N-doped biochar [30]. Nitrogen content in N-doped biochar catalyst after catalytic pyrolysis decreased a little It was due to that bamboo catalytic pyrolysis generated some biochar product with lower nitrogen content, and it mixed with N-doped biochar catalyst, thus nitrogen in N-doped biochar catalyst would be diluted, leading to the decrease of nitrogen. And hydrogen content decreased a little from ~2.5 wt.% (Hydrogen content of biochar product from bamboo pyrolysis was also ~2.5 wt.%) to ~2.3 wt.%, which may be ascribed to the H-donors effect of N-doped biochar catalyst during catalytic pyrolysis process [18]. It was also consistent with the higher phenols content (see Figure 4).

Furthermore, the S_{BET} and V_{total} of biochar and N-doped biochar catalysts also decreased largely compared with those of fresh catalysts, while average pore diameter increased accordingly. It was mainly attributed to that bamboo catalytic pyrolysis generated some biochar product with lower S_{BET} and V_{total}, which mixed with catalyst after catalytic pyrolysis, leading to the decrease of S_{BET} and V_{total}. Another reason may be that the carbon deposition during catalytic pyrolysis process condensed on the surface of catalyst. It blocked some micropores, and led to the decrease of S_{BET} and V_{total} and the increase of pore size [58, 59]. From SEM micrographs (Figure S3), it could be found that the porous structure of N-doped biochar was still more developed than that of biochar. However, the surface of biochar and N-doped biochar became more smooth, and the pores on the surface decreased largely, compared with that before catalytic pyrolysis, perhaps due to the carbon deposition. It is consistent with the results of Table 2.

To further reveal the catalytic pyrolysis mechanism of N-doped biochar catalyst, the O- and N-containing groups evolution of N-doped biochar catalyst after catalytic pyrolysis was explored in depth, shown as Figure 5. After the catalytic pyrolysis, O-containing groups on the surface of biochar catalyst showed great change (Figure 5a), where O-C=O/C-O became the main O-

containing groups. From the absolute content of O-containing groups (Figure 5d, determined through oxygen content in biochar and relative content of O-containing groups on the surface of biochar), it could be found that C=O groups decreased largely, while O-C=O, C-O, -OH and -COOH groups increased significantly, especially O-C=O/C-O groups. Being different with biochar catalyst, for N-doped biochar catalyst, O-containing groups in the solid char after catalytic pyrolysis cannot be viewed to completely come from N-doped biochar catalyst, as bamboo feedstock contained large amounts of oxygen, and some of them would retain in biochar product after pyrolysis. Thus, in order to understand the evolution of O-containing groups on the surface of N-doped biochar catalyst. We also compared the O-containing groups on char product from individual pyrolysis of bamboo (That is biochar catalyst) with N-doped biochar catalyst. It could be found that, C=O groups were the highest O-containing groups for biochar and N-doped biochar catalyst before catalytic pyrolysis. After catalytic pyrolysis, the main O-containing groups of N-doped biochar catalysts became O-C=O/-OH groups (Figure 5b, different catalyst showed similar change tendency, here just biochar-N30 after catalytic pyrolysis is shown, others are shown in Figure S4), and the absolute content of all O-containing groups decreased largely, especially C=O groups, which became the lowest O-containing groups from the highest one (Figure 5d). The great decrease of C=O groups may be attributed to water and organic intermediates from bamboo pyrolysis reacting with C=O groups through decarboxylation reactions. While other O-containing groups mainly acted as catalyst and reactant, which could catalyse conversion of pyrolytic intermediates and react with intermediates to form phenols and aromatics [60].
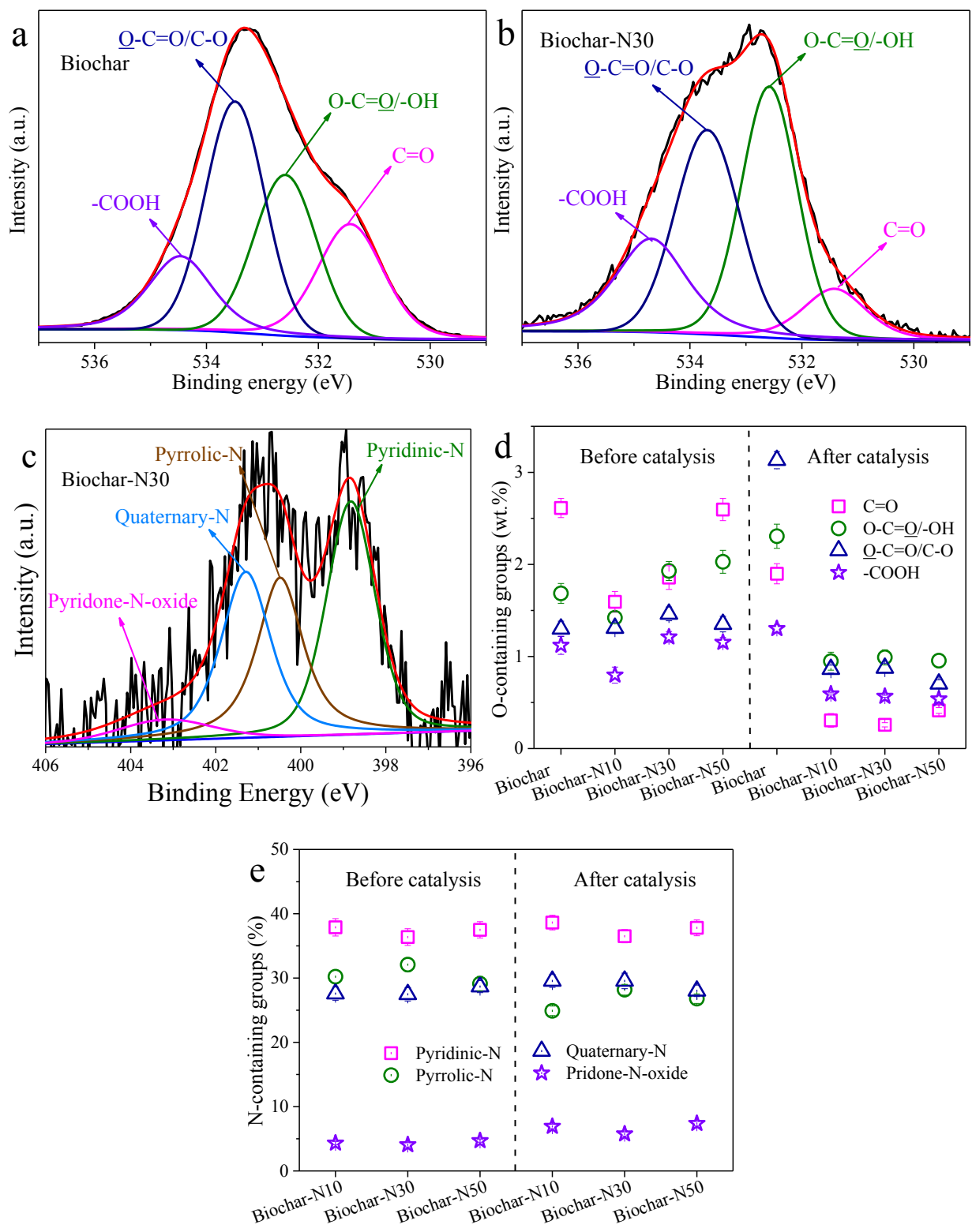
Figure 5. N- and O-containing groups in biochar and N-doped biochar after catalytic pyrolysis.

The N-containing groups on the surface of N-doped biochar catalyst after catalytic pyrolysis showed no obvious change, and the main N-containing groups were still pyridinic-N, pyrrolic-N and quanternary-N with little pyridone-N-oxide (Figure 5c, only biochar-N30 after catalytic pyrolysis is shown here, as others showed similar change tendency, shown as Figure S4), also indicating the good stability of N-containing groups in N-doped biochar catalyst. It should be pointed out that, the N-containing groups in solid char were considered to come from the N-doped biochar catalyst, as nitrogen content in bamboo feedstock is so low, which could be ignored almost. Moreover, only relative content, but not absolute yield, of N-containing groups in N-doped biochar pre and after catalytic pyrolysis is shown here (Figure 5e), as N-containing groups would be diluted after catalytic pyrolysis. N-containing groups in N-doped biochar catalyst mainly acted as adsorbent and catalyst (pyridinic-N and pyrrolic-N possessed high catalytic activity) [29], which could adsorb pyrolytic intermediates and catalyse conversion of them into phenols. Besides, it could be found that pyrrolic-N content decreased a little, while quaternary-N increased accordingly, which may be due to that a little pyrrolic-N converted to quaternary-N after hydrogen supply reactions.

In particular, the decrease of O-containing groups of N-doped biochar catalyst was much larger than that of biochar catalyst. It may be due to that N-doped biochar catalyst contained developed porous structure, and abundant active N-containing groups. They showed alkaline, and could effectively adsorb more water and other pyrolytic intermediates (weak acidity), then promoted them to react with active O-containing groups, leading to the great decrease of O-containing groups in N-doped biochar catalyst. It may also be the reason why N-doped biohcar catalyst showed stronger catalytic activity [18, 61].

Besides, considering the possible nitrogen emission during catalytic pyrolysis with N-doped biochar, for greener utilization of N-doped biochar catalyst, nitrogen recovery is shown in Figure 6. It could be found that the nitrogen recovery for different N-doped biochar was higher than 94 wt.%, but a little lower than 100%, perhaps due to the little nitrogen releasing during bamboo pyrolysis itself, indicating the excellent recovery effect and almost no nitrogen emission. It also indicated that the N-containing groups in N-doped biochar was very stable during biomass catalytic pyrolysis. Furthermore, N-doped biochar after catalytic pyrolysis still possessed higher nitrogen content, stably active N-containing groups, and larger surface area. It indicated that N-doped biochar could have the potential to be recycled. While the life time property would be investigated in detail in the coming future.
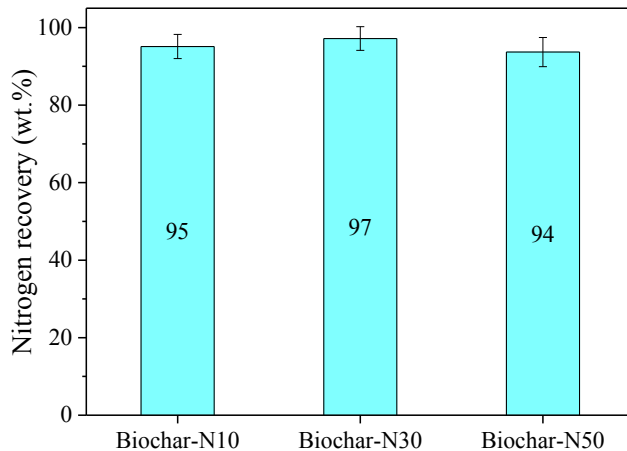

Figure 6. Nitrogen recovery during catalytic pyrolysis with N-doped biochar catalyst.

3.5. Catalytic pyrolysis mechanism of N-doped biochar catalyst

Based on above discussion, the possible catalytic pyrolysis mechanism of N-doped biochar catalyst is shown in Figure 7. During catalytic pyrolysis process, N-doped biochar catalyst acted as an adsorbent firstly (adsorption process). The N-containing groups in N-doped biochar showed alkaline property, which could effectively adsorb most of pyrolytic intermediates from bamboo pyrolysis. Then N-doped biochar catalyst would act as a catalyst (catalytic process). Active N- and

O-containing groups in N-doped biochar would catalyse conversion of the pyrolytic intermediates. Carbon atoms next to pyridinic-N with Lewis basicity were the active sites [62, 63], which could significantly promote the generation of phenols. Pyrrolic-N could provide hydrogen for H-acceptors (such as radicals of 4-vinyl phenol, 4-ethyl phenol, p-cresol, phenol) to promote the formation of phenols (Figure 4). –COOH, O-C=O, and –OH groups had catalytic effect on O-species intermediates for the generation of phenols and aromatics. N-doped biochar catalyst also promoted the reactions between phenols intermediates (H-acceptors) and O-species (H-donors) adsorbed in N-doped biochar to form more phenols through dehydration reactions. Moreover, C=O groups (acted as a reactant) could combine with water to form –COOH groups, then undergo decarboxylation reactions (release out CO_2), which was also consistent with the increase of CO_2 in gaseous product (Figure 3).

As C=O groups in N-doped biochar catalyst decreased most largely, C=O groups reacting with water may be important reaction pathways. The detailed reaction pathways of C=O groups and H_2O were explored in depth based on experiment results and quantum calculations, shown as Figure S5. Two possible C=O type unit R1 and R2 were selected as model compounds for N-doped biochar. Path-a was designed to show direct cleavage of the C=O group R1 without H_2O, whereas Path-b and Path-c were designed to illustrate the role of H_2O in the cleavage of C=O groups. During the process of biomass catalytic pyrolysis with N-doped biochar catalyst, the dehydration of cellulose and hemicellulose produced a large amount of water, which can enter the N-doped biochar pores (showed alkaline, and could effectively adsorb H_2O) and easily react with C=O groups via pathways similar to Path-b and Path-c, thereby promoted the C=O group removal in N-doped biochar and the formation of CO_2.
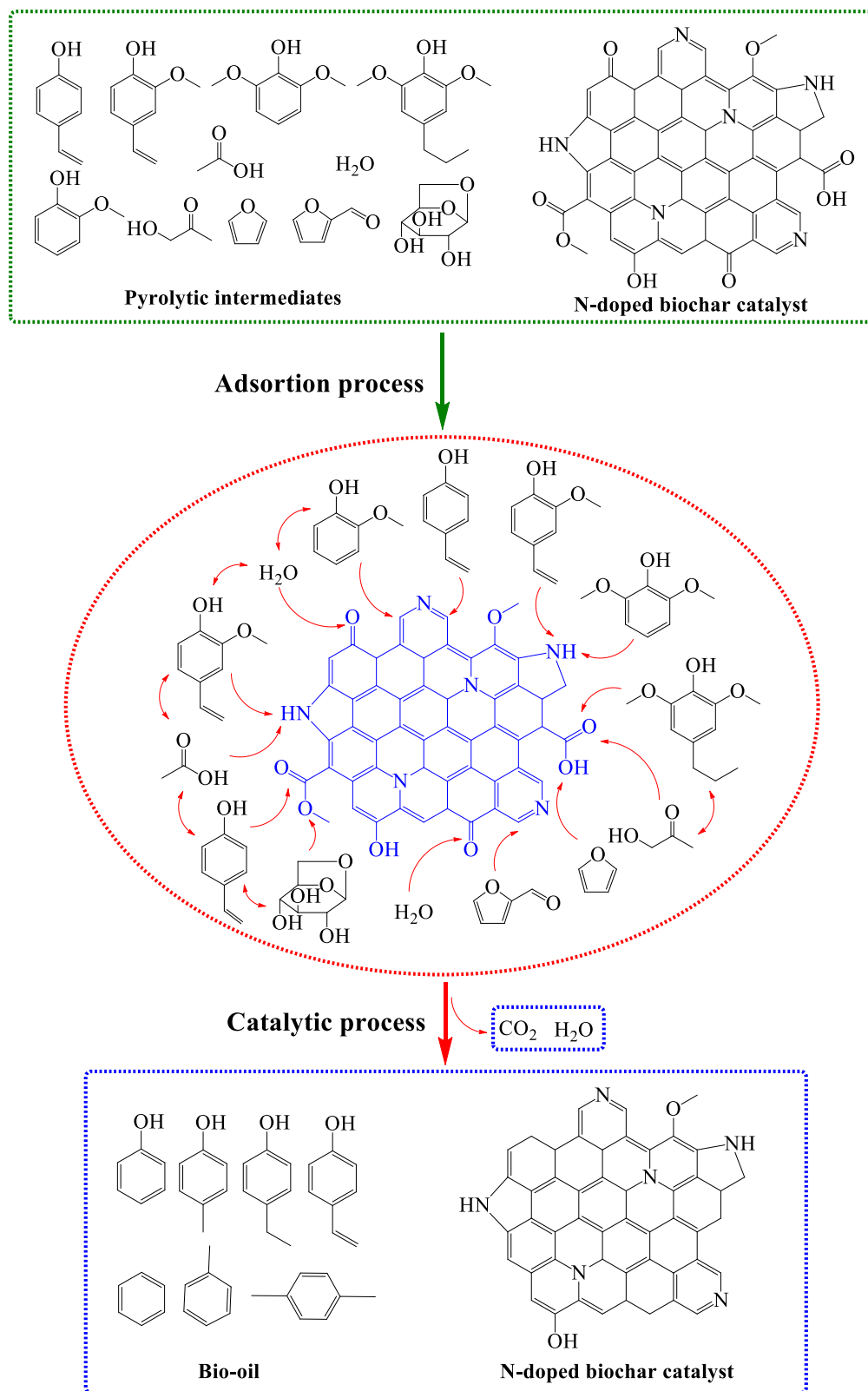
Figure 7. The possible catalytic pyrolysis mechanism of N-doped biochar catalyst.

In addition, the possible formation pathways of 4-vinyl phenol (the dominant phenol) are shown as Figure 8. N-doped biochar provided large amounts of H free radicals, and promoted the cleavage of β-O-4 and dehydration reactions in lignin firstly, which formed a number of p-coumaryl, coniferyl and sinapyl alcohol subunits intermediates, then these intermediates converted to 4-vinyl phenol with methoxyl through removing –CH_2-OH groups, at last they further removed –O-CH_3 groups and formed 4-vinyl phenol [64-66]. It indicated that N-doped biochar catalyst could promote the generation of phenols from bamboo catalytic pyrolysis, especially valuable 4-vinyl phenol.
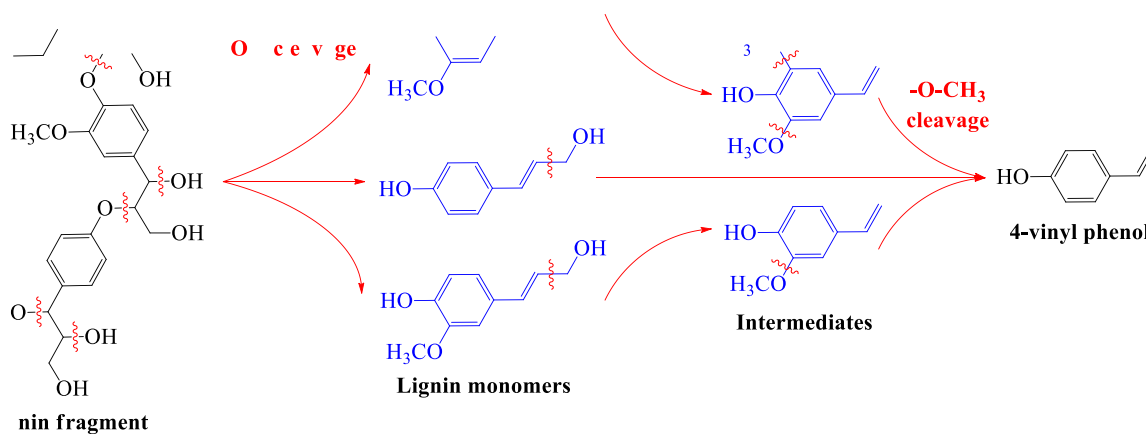

Figure 8. The possible formation pathways of 4-vinyl phenol during catalytic pyrolysis with N-doped biochar catalyst.

4. Conclusions

Bamboo wastes catalytic pyrolysis with N-doped biochar catalyst for phenols products was studied to explore the catalytic pyrolysis mechanism of N-doped biochar catalyst. Results showed that N-doped biochar catalyst greatly promoted the generation of phenols (reached 82%), while inhibited the formation of O-species and acetic acid, with more CO_2 and H_2O release. Valuable 4-vinyl phenol was the main phenols product with 31% content and 6.65 wt.% yield, as well as 16%

4-ethyl phenol, 9% p-cresol, and 7% phenol with the yield of 3.04 wt.%, 1.83 wt.%, and 1.24 wt.%, respectively. N-doped biochar acted as adsorbent, catalyst, reactant during catalytic pyrolysis. The alkaline N-containing groups adsorbed pyrolytic intermediates firstly on the surface of N-doped biochar, then active N- and O-containing groups catalysed conversion of them or reacted with them to form phenols and aromatics, which greatly improved the quality of bio-oil. Thus, biomass catalytic pyrolysis with N-doped biochar catalyst was a promising method for realizing the green and valuable utilization of biomass resource.

References

[1] Wang S, Dai G, Yang H, Luo Z. Lignocellulosic biomass pyrolysis mechanism: A state-of-the-art review. Prog Energy Combust Sci 2017;62:33-86.

[2] Alonso DM, Hakim SH, Zhou S, Won W, Hosseinaei O, Tao J, et al. Increasing the revenue from lignocellulosic biomass: Maximizing feedstock utilization. Sci Adv 2017;3,e1603301.

[3] Qi X, Fan W. Selective production of aromatics by catalytic fast pyrolysis of furan with in situ dehydrogenation of propane. ACS Catal 2019;9:2626-32.

[4] Zhou X, Li W, Mabon R, Broadbelt LJ. A mechanistic model of fast pyrolysis of hemicellulose. Energ Environ Sci 2018;11:1240-60.

[5] Yang H, Coolman R, Karanjkar P, Wang H, Dornath P, Chen H, et al. The effects of contact time and coking on the catalytic fast pyrolysis of cellulose. Green Chem 2017;19:286-97.

[6] Yang H, Coolman RJ, Karanjkar P, Wang H, Xu Z, Chen H, et al. The effect of steam on the catalytic fast pyrolysis of cellulose. Green Chem 2015;17:2912-23.

[7] Huber GW, Iborra S, Corma A. Synthesis of transportation fuels from biomass: Chemistry, catalysts, and engineering. Chem Rev 2006;106:4044-98.

[8] Liu C, Wang H, Karim AM, Sun J, Wang Y. Catalytic fast pyrolysis of lignocellulosic biomass. Chem Soc Rev 2014;43:7594-623.

[9] Gallezot P. Conversion of biomass to selected chemical products. Chem Soc Rev 2012;41:1538-58.

[10] Zhou CH, Xia X, Lin CX, Tong DS, Beltramini J. Catalytic conversion of lignocellulosic biomass to fine chemicals and fuels. Chem Soc Rev 2011;40:5588-617.

[11] Schobert HH, Song C. Chemicals and materials from coal in the 21st century. Fuel 2002;81:15-32.

[12] Lochab B, Shukla S, Varma IK. Naturally occurring phenolic sources: monomers and polymers. Rsc Adv 2014;4:21712-52.

[13] Amen-Chen C, Pakdel H, Roy C. Production of monomeric phenols by thermochemical conversion of biomass: a review. Bioresour Technol 2001;79:277-99.

[14] Kim J-S. Production, separation and applications of phenolic-rich bio-oil – A review. Bioresour Technol 2015;178:90-8.

[15] Naron DR, Collard FX, Tyhoda L, Görgens JF. Production of phenols from pyrolysis of sugarcane bagasse lignin: Catalyst screening using thermogravimetric analysis – Thermal

desorption – Gas chromatography – Mass spectroscopy. J. Anal Appl Pyrolysis 2019;138:120-31.

[16] Peng C, Zhang G, Yue J, Xu G. Pyrolysis of lignin for phenols with alkaline additive. Fuel Process Technol 2014;124:212-21.

[17] Lu Q, Zhang Z, Yang X, Dong C, Zhu X. Catalytic fast pyrolysis of biomass impregnated with K_3PO_4 to produce phenolic compounds: Analytical Py-GC/MS study. J Anal Appl Pyrolysis 2013;104:139-45.

[18] Lu Q, Ye X, Zhang Z, Cui M, Guo H, Qi W, et al. Catalytic fast pyrolysis of bagasse using activated carbon catalyst to selectively produce 4-ethyl phenol. Energ Fuel 2016;30:10618-26.

[19] Yang Z, Lei H, Zhang Y, Qian K, Villota E, Qian M, et al. Production of renewable alkyl-phenols from catalytic pyrolysis of Douglas fir sawdust over biomass-derived activated carbons. Appl Energy 2018;220:426-36.

[20] Zhang Y, Lei H, Yang Z, Qian K, Villota E. Renewable high-purity mono-phenol production from catalytic microwave-induced pyrolysis of cellulose over biomass-derived activated carbon catalyst. ACS Sustain Chem Eng 2018;6:5349-57.

[21] Mamaeva A, Tahmasebi A, Tian L, Yu J. Microwave-assisted catalytic pyrolysis of lignocellulosic biomass for production of phenolic-rich bio-oil. Bioresour Technol 2016;211:382-9.

[22] Bu Q, Lei H, Wang L, Wei Y, Zhu L, Zhang X, et al. Bio-based phenols and fuel production from catalytic microwave pyrolysis of lignin by activated carbons. Bioresour Technol 2014;162:142-7.

[23] Chen W, Li K, Xia M, Chen Y, Yang H, Chen Z, et al. Influence of NH_3 concentration on biomass nitrogen-enriched pyrolysis. Bioresour Technol 2018;263:350-7.

[24] Chen W, Chen Y, Yang H, Li K, Chen X, Chen H. Investigation on biomass nitrogen-enriched pyrolysis: Influence of temperature. Bioresour Technol 2018;249:247-53.

[25] Chen W, Yang H, Chen Y, Chen X, Fang Y, Chen H. Biomass pyrolysis for nitrogen-containing liquid chemicals and nitrogen-doped carbon materials. J Anal Appl Pyrolysis 2016;120:186-93.

[26] Ahmad FB, Zhang Z, Doherty WOS, O'Hara IM. The outlook of the production of advanced fuels and chemicals from integrated oil palm biomass biorefinery. Renew Sust Energy Rev 2019;109:386-411.

[27] Serp P, Machado B, Nanostructured carbon materials for catalysis, Royal Society of Chemistry2015.

[28] Figueiredo JL, Pereira MFR. The role of surface chemistry in catalysis with carbons. Catal Today 2010;150:2-7.

[29] Li M, Xu F, Li H, Wang Y. Nitrogen-doped porous carbon materials: promising catalysts or catalyst supports for heterogeneous hydrogenation and oxidation. Catal Sci Technol 2016;6:3670-93.

[30] Chen W, Li K, Xia M, Yang H, Chen Y, Chen X, et al. Catalytic deoxygenation co-pyrolysis of bamboo wastes and microalgae with biochar catalyst. Energy 2018;157:472-82.

[31] Goering HK, Van Soest PJ. Forage fiber analyses (apparatus, reagents, prcedures, and some applications). USDA Agr Handb 1970.

[32] Van Soest PJ. Use of detergents in the analysis of fibrous feeds. 2. A rapid method for the determination of fiber and lignin. J Assoc Off Agr Chem 1963;46:829-35.

[33] Frisch MJ, Schlegel HB, Scuseria GE, Robb MA, Cheeseman JR, Scalmani G, et al. Gaussian 09 Revision D.01, Gaussian, Inc., Wallingford CT, 2009.

[34] Canneaux S, Bohr F, Henon E. KiSThelP: A program to predict thermodynamic properties and rate constants from quantum chemistry results. J Comput Chem 2014;35:82-93.

[35] Alecu IM, Zheng J, Zhao Y, Truhlar DG. Computational thermochemistry: Scale factor databases and scale factors for vibrational frequencies obtained from electronic model chemistries. J Chem Theory and Comput 2010;6:2872-87.

[36] Zhang Y, Duan D, Lei H, Villota E, Ruan R. Jet fuel production from waste plastics via catalytic pyrolysis with activated carbons. Appl Energy 2019;251:113337.

[37] Zhao Y, Feng D, Zhang Y, Huang Y, Sun S. Effect of pyrolysis temperature on char structure and chemical speciation of alkali and alkaline earth metallic species in biochar. Fuel Process Technol 2016;141, Part 1:54-60.

[38] Zhou JH, Sui ZJ, Zhu J, Li P, Chen D, Dai YC, et al. Characterization of surface oxygen complexes on carbon nanofibers by TPD, XPS and FT-IR. Carbon 2007;45:785-96.

[39] Wang K, Jiang P, Yang M, Ma P, Qin J, Huang X, et al. Metal-free nitrogen -doped carbon nanosheets: a catalyst for the direct synthesis of imines under mild conditions. Green Chem 2019;21:2448-61.

[40] Lam E, Luong JHT. Carbon materials as catalyst supports and catalysts in the transformation of biomass to fuels and chemicals. ACS Catal 2014;4:3393-410.

[41] Wang N, Chen D, Arena U, He P. Hot char-catalytic reforming of volatiles from MSW pyrolysis. Appl Energy 2017;191:111-24.

[42] Yang H, Yan R, Chen H, Lee DH, Zheng C. Characteristics of hemicellulose, cellulose and lignin pyrolysis. Fuel 2007;86:1781-8.

[43] Bu Q, Lei H, Wang L, Wei Y, Zhu L, Liu Y, et al. Renewable phenols production by catalytic microwave pyrolysis of Douglas fir sawdust pellets with activated carbon catalysts. Bioresour Technol 2013;142:546-52.

[44] Patel M, Kumar A. Production of renewable diesel through the hydroprocessing of lignocellulosic biomass-derived bio-oil: A review. Renew Sust Energy Rev 2016;58:1293-307.

[45] Chen WH, Lin YY, Liu HC, Chen TC, Hung CH, Chen CH, et al. A comprehensive analysis of food waste derived liquefaction bio-oil properties for industrial application. Appl Energy 2019;237:283-91.

[46] Yang H, Huan B, Chen Y, Gao Y, Li J, Chen H. Biomass-based pyrolytic polygeneration system for bamboo industry waste: Evolution of the char structure and the pyrolysis mechanism. Energ Fuel 2016;30:6430-9.

[47] Groen JC, Zhu W, Brouwer S, Huynink SJ, Kapteijn F, Moulijn JA, et al. Direct demonstration of enhanced diffusion in mesoporous ZSM-5 zeolite obtained via controlled desilication. J Am Chem Soc 2007;129:355-60.

[48] Bu Q, Lei H, Ren S, Wang L, Zhang Q, Tang J, et al. Production of phenols and biofuels by catalytic microwave pyrolysis of lignocellulosic biomass. Bioresour Technol 2012;108:274-9.

[49] Zhang Z, Lu Q, Ye X, Li W, Hu B, Dong C. Production of phenolic-rich bio-oil from catalytic fast pyrolysis of biomass using magnetic solid base catalyst. Energy Convers Manage 2015;106:1309-17.

[50] Gayubo AG, Aguayo AT, Atutxa A, Aguado R, Bilbao J. Transformation of oxygenate components of biomass pyrolysis oil on a HZSM-5 zeolite. I. Alcohols and phenols. Ind Eng Chem Res 2004;43:2610-8.

[51] Fanchiang WL, Lin YC. Catalytic fast pyrolysis of furfural over H-ZSM-5 and Zn/H-ZSM-5 catalysts. Appl Catal A-Gen. 2012;419-420:102-10.

[52] Patwardhan PR, Brown RC, Shanks BH. Understanding the fast pyrolysis of lignin. ChemSusChem 2011;4:1629-36.

[53] Cordella M, Torri C, Adamiano A, Fabbri D, Barontini F, Cozzani V. Bio-oils from biomass slow pyrolysis: A chemical and toxicological screening. J Hazard Mater 2012;231-232:26-35.

[54] Zhang Z, Lu Q, Ye X, Li W, Zhang Y, Dong C. Selective production of 4-ethyl phenol from low-temperature catalytic fast pyrolysis of herbaceous biomass. J Anal Appl Pyrolysis 2015;115:307-15.

[55] Qu YC, Wang Z, Lu Q, Zhang Y. Selective production of 4-vinylphenol by fast pyrolysis of herbaceous biomass. Ind Eng Chem Res 2013;52:12771-6.

[56] Anca-Couce A. Reaction mechanisms and multi-scale modelling of lignocellulosic biomass pyrolysis. Prog Energy Combust Sci 2016;53:41-79.

[57] Ravenni G, Elhami OH, Ahrenfeldt J, Henriksen UB, Neubauer Y. Adsorption and decomposition of tar model compounds over the surface of gasification char and active carbon within the temperature range 250–800°C. Appl Energy 2019;241:139-51.

[58] Dawodu FA, Ayodele O, Xin J, Zhang S, Yan D. Effective conversion of non-edible oil with high free fatty acid into biodiesel by sulphonated carbon catalyst. Appl Energy 2014;114:819-26.

[59] Hervy M, Weiss-Hortala E, Pham Minh D, Dib H, Villot A, Gérente C, et al. Reactivity and deactivation mechanisms of pyrolysis chars from bio-waste during catalytic cracking of tar. Appl Energy 2019;237:487-99.

[60] Omoriyekomwan JE, Tahmasebi A, Yu J. Production of phenol-rich bio-oil during catalytic fixed-bed and microwave pyrolysis of palm kernel shell. Bioresour Technol 2016;207:188-96.

[61] Mukarakate C, McBrayer JD, Evans TJ, Budhi S, Robichaud DJ, Iisa K, et al. Catalytic fast pyrolysis of biomass: the reactions of water and aromatic intermediates produces phenols. Green Chem 2015;17:4217-27.

[62] Guo D, Shibuya R, Akiba C, Saji S, Kondo T, Nakamura J. Active sites of nitrogen-doped carbon materials for oxygen reduction reaction clarified using model catalysts. Science 2016;351:361-5.

[63] She Y, Chen J, Zhang C, Lu Z, Ni M, Sit PHL, et al. Nitrogen-doped graphene derived from ionic liquid as metal-free catalyst for oxygen reduction reaction and its mechanisms. Appl Energy 2018;225:513-21.

[64] Ojha DK, Viju D, Vinu R. Fast pyrolysis kinetics of alkali lignin: Evaluation of apparent rate parameters and product time evolution. Bioresour Technol 2017;241:142-51.

[65] Shuai L, Amiri MT, Questell-Santiago YM, Héroguel F, Li Y, Kim H, et al. Formaldehyde stabilization facilitates lignin monomer production during biomass depolymerization. Science 2016;354:329-33.

[66] Li Y, Demir B, Vázquez Ramos LM, Chen M, Dumesic JA, Ralph J. Kinetic and mechanistic insights into hydrogenolysis of lignin to monomers in a continuous flow reactor. Green Chem 2019.